

# An Iterative Spectral-Spatial Bayesian Labeling Approach For Unsupervised Robust Change Detection On Remotely Sensed Multispectral Imagery

RAFAEL WIEMKER

Universität Hamburg, II. Institut für Experimentalphysik  
D-22761 Hamburg, Germany; wiemker@informatik.uni-hamburg.de  
kogs-www.informatik.uni-hamburg.de/projects/Censis.html

**Abstract** In multispectral remote sensing, change detection is a central task for all kinds of monitoring purposes. We suggest a novel approach where the problem is formulated as a Bayesian labeling problem. Considering two registered images of the same scene but different recording time, a Bayesian probability for 'Change' and 'NoChange' is determined for each pixel from spectral as well as spatial features. All necessary parameters are estimated from the image data itself during an iterative clustering process which updates the current probabilities. The contextual spatial features are derived from Markov random field modeling. We define a potential as a function of the probabilities of neighboring pixels to belong to the same class.

The algorithm is robust against spurious change detection due to changing recording conditions and slightly misregistered high texture areas. It yields successful results on simulated and real multispectral multitemporal aerial imagery.

## 1 Introduction

In the field of multispectral remote sensing, change detection is a central task for all monitoring purposes. It uses multitemporal imagery in order to detect land cover changes caused by short-term phenomena such as flooding and seasonal vegetation change, or long-term phenomena such as urban development and deforestation [5,6].

In general, remotely sensed multispectral imagery for monitoring purposes is recorded by overflights over the same land area at two times,  $T_1$  and  $T_2$ , say. An appropriate algorithm must then compare the two observed images of the same scene and assist the analyst by designating those areas where the ground cover has apparently changed. For specific applications, certain wavelength bands may be selected, whereas for general purpose monitoring, all spectral bands will be taken into account.

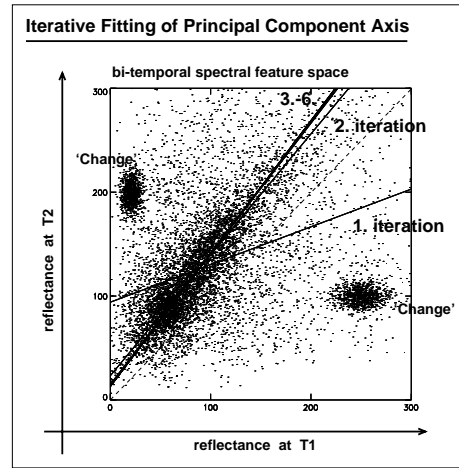
A pre-requisite to pixel-wise change detection is the registration between the two images which are to be compared. The registration can be carried out either by geocoding of both images or by direct image-to-image registration. Imagery from airborne scanners in general requires locally adaptive coordinate transformation functions as described in [8].

The general problem is to compare two images  $I_1$  and  $I_2$  of the same scene recorded at times  $T_1$  and  $T_2$ . When using a multispectral sensor with  $n$  spectral bands denoted

by index  $i = 1 \dots n$ , we particularly want to compare the spectral values  $x_i(T_1)$  and  $x_i(T_2)$  for a certain pixel  $\mathbf{x}$ . Depending on the spectral differences and contextual considerations, a decision is sought whether this pixel shows a ground surface patch which – with respect to its ground cover type – has either changed or has remained unchanged.

## 2 Known Problems and Here Chosen Approaches

### 2.1 Iterative, Principal Component Based Change Detection



A fundamental problem of comparing two images of the same scene is that the recording conditions may have changed. In particular, the direct solar illumination and the diffuse sky light, the path radiance, and the transmittance of the atmosphere, as well as the dark current and gain setting of the sensor may have changed individually in each spectral band. All these topics can roughly be categorized into influencing the received spectral signal in either a multiplicative or an additive fashion. Thus the relation between the spectral signal  $x_i(T_1)$  and  $x_i(T_2)$  received from a certain Lambertian reflecting surface at two times  $T_1$

and  $T_2$  is very often modeled approximately as a linear function [5,6].

Let us consider a bi-temporal feature space for a single spectral band  $i$  where each pixel  $\mathbf{x}$  is denoted by a point  $\mathbf{x}_i = [x_i(T_1), x_i(T_2)]^T$ . Then, as a consequence of the assumed linear relation between unchanged pixels, we expect all unchanged pixels to lie in a narrow elongated cluster along a principal axis. On the other hand, the pixels which do have experienced 'change' in their spectral appearance are expected to lie far out from this axis [5]. Thus, the amount of 'change' is quantified by the magnitude of the second principal component (PC):  $c'_i(\mathbf{x}_i) = g_{1,i}(x_i(T_1) - m_{i,1}) + g_{2,i}(x_i(T_2) - m_{i,2})$  where  $\mathbf{g}_i = [g_{1,i}, g_{2,i}]^T$  is the second eigenvector of the overall covariance matrix  $\mathbf{C}_i$  ( $2 \times 2$  matrix), and  $\mathbf{m}_i = [m_{1,i}, m_{2,i}]^T$  are the mean values of  $x_i(T_1)$  and  $x_i(T_2)$ .

An obvious problem with principal component based change detection is that the principal components are conventionally estimated as the eigenvectors of the covariance matrix  $\mathbf{C}_i$  computed from all pixels  $\mathbf{x}_i$ , including those which have experienced 'change'. Thus, the such found 'NoChange'-axis is prone to error. In our iterative approach the problem is addressed such that the cluster mean  $\mathbf{m}_i$  and the covariance matrix  $\mathbf{C}_i$  are determined from all pixels  $\mathbf{x}$  but weighted with their respective probabilities  $P(\text{NC}|\mathbf{x})$  to be 'NoChange'-pixels.

## 2.2 Avoiding Spurious Change Detection in High Texture Areas

A typical problem of remotely sensed imagery is that the registration of airborne scanner imagery only yields registration accuracies of some pixels at best. In image areas of high texture, even small misregistration errors will cause a large amount of spurious 'Change': If *e.g.* a test image is shifted by one pixel and subtracted from the original image, we essentially observe a crude edge detector which enhances all contours of the image. In order to avoid this effect, a crucial provision of our approach is to normalize all change components  $c'_i(\mathbf{x}_i)$  by the combined local variance  $\sigma_{\text{loc},i}^2(\mathbf{x})$ :

$$c_i(\mathbf{x}_i) = c'_i(\mathbf{x}_i) / \sqrt{\sigma_{\text{loc},i}^2(\mathbf{x})} \quad (1)$$

The local variance  $\sigma_{\text{loc},i}^2(\mathbf{x})$  is estimated from the spectral variances (mean square scatter)  $\sigma_{\text{loc},I_1,i}^2(\mathbf{x})$  and  $\sigma_{\text{loc},I_2,i}^2(\mathbf{x})$  in the local neighborhood  $\mathcal{N}(\mathbf{x})$  of pixel  $\mathbf{x}$  in image  $I_1$  and image  $I_2$  in spectral band  $i$ . Here we define the local neighborhood  $\mathcal{N}(\mathbf{x})$  as the  $k \times k$  window centered around the pixel  $\mathbf{x}$ , excluding the pixel  $\mathbf{x}$  itself. Error propagation yields that after the PC-transformation the errors  $\sigma_{\text{loc},I_1,i}^2(\mathbf{x})$  and  $\sigma_{\text{loc},I_2,i}^2(\mathbf{x})$  yield a combined error of  $\sigma_{\text{loc},i}^2(\mathbf{x}) = g_{1,i}^2 \sigma_{\text{loc},I_1,i}^2(\mathbf{x}) + g_{2,i}^2 \sigma_{\text{loc},I_2,i}^2(\mathbf{x})$ . The normalization of the change component with the estimated local variance means that the spectral values  $x_i(T_1)$  and  $x_i(T_2)$  should only then be considered as indicating 'Change' if their difference is large in comparison to the variances in their respective neighborhoods, since otherwise the difference can be explained as a small shift of a textured surface.

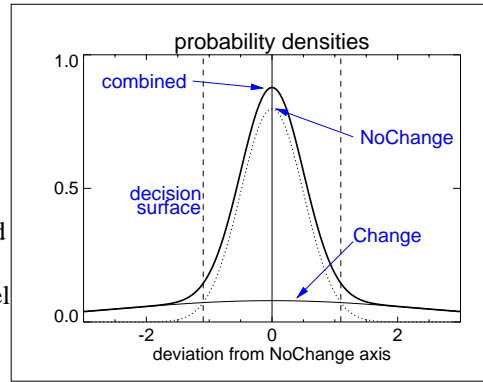
## 2.3 Bayesian Decision on 'Change' vs. 'NoChange'

Conventional change detection depends crucially on the setting of threshold parameters by the analyst. In each spectral band  $i$ , it has to be decided just when the change component  $c_i(\mathbf{x}_i)$  of a given pixel  $\mathbf{x}$  is large enough to be considered 'Change'.

The unsupervised approach presented here considers change detection as a Bayesian labeling problem, where each pixel is assigned to one out of two classes  $\omega = \{\text{CH}, \text{NC}\}$ : 'Change' or 'NoChange'.

This decision is made using *Bayes Rule*,

which minimizes the probability of error [2]: The pixel is assigned to the class  $\omega$  which has the maximum *a posteriori* probability  $P(\omega|\mathbf{x})$ . This probability is given by the normalized product of the *a priori* probability and the conditional probability density computed from the observation  $\mathbf{x}$ . We assume that the *a priori* probability for class  $\omega$  is proportional to the relative abundance  $N_\omega/N_{\text{tot}}$ , where  $N_{\text{tot}} = \sum_\omega N_\omega$  is the total number of pixels and  $N_\omega$  the sum of the probabilities of class  $\omega$  over all pixels:



$N_\omega = \sum_{\mathbf{x}} P(\omega|\mathbf{x})$ . The normalized conditional probability density derived from *spectral features* in spectral band  $i$  is

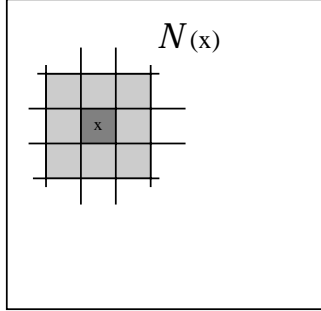
$$p_i(\mathbf{x}_i|\omega) = \frac{1}{\sqrt{2\pi\sigma_{\omega,i}^2}} \exp\left(-\frac{1}{2} \frac{c_i(\mathbf{x}_i)^2}{\sigma_{\omega,i}^2}\right) \quad ; \quad \text{with} \quad \int_{-\infty}^{\infty} p_i dc_i = 1 \quad (2)$$

and is multiplied with the respective probability densities of the other spectral bands. This tacitly assumes a Gaussian distribution of the 'Change'-components  $c_i(\mathbf{x}_i)$ . The within-class-variances  $\sigma_{\omega,i}^2$  are estimated from the data itself during the iteration. This kind of unsupervised iterative clustering of unlabeled data is described *e.g.* in [2]. The variance of a class  $\omega$  with respect to the variable  $c_i(\mathbf{x}_i)$  is estimated from all pixels  $\mathbf{x}$  weighted with their respective probability  $P(\omega|\mathbf{x})$ : The conditional probability density  $p_{\text{con}}(\mathbf{x}|\omega)$  derived from *context features* is described in Section 2.4.

Finally, the *a posteriori* probability is the product of *a priori* probability and the spectral and spatial conditional probabilities. It is normalized by the sum of the probability densities for all classes  $\omega$  in order to be constrained to the interval  $P(\omega|\mathbf{x}) \in [0 \dots 1]$  and to add up to unity:  $\sum_{\omega} P(\omega|\mathbf{x}) = 1$ . Hence, our overall *a posteriori* probability amounts to

$$P(\omega|\mathbf{x}) = \frac{N_\omega/N \cdot p_{\text{con}}(\mathbf{x}|\omega) \cdot \prod_i p_i(\mathbf{x}_i|\omega)}{\sum_{\omega} [N_\omega/N \cdot p_{\text{con}}(\mathbf{x}|\omega) \cdot \prod_i p_i(\mathbf{x}_i|\omega)]} \quad (3)$$

#### 2.4 Context Features derived from Markov Random Field Modeling



The Markovian property means that the probability of pixel  $\mathbf{x}$  to belong to class  $\omega$  is influenced by and only by the classes assigned to the pixels  $\mathbf{x}'$  in its neighborhood  $\mathcal{N}(\mathbf{x})$  [4]. Here we define  $\mathcal{N}$  as the quadrangular  $k \times k$  window around the pixel  $\mathbf{x}$ , excluding  $\mathbf{x}$  itself. MRF-based approaches to contextually enhanced multispectral classification have recently been used in remote sensing [3,7]. Unlike these approaches we here use a contextual potential function  $U(\mathbf{x}|\omega)$  which not only evaluates identical or different labels in the neighborhood  $\mathcal{N}$  with a  $\{0,1\}$ -Kronecker-function, but which is influenced continuously by the current probabilities of the neighboring pixels:

$$p_{\text{con}}(\mathbf{x}|\omega) = \frac{1}{Z} \exp(-\beta U(\mathbf{x}|\omega)) \quad \text{with} \quad U(\mathbf{x}|\omega) = \sum_{\mathbf{x}' \in \mathcal{N}(\mathbf{x})} [1 - P(\omega|\mathbf{x}')] \quad (4)$$

Then the context-conditional probability  $p_{\text{con}}(\mathbf{x}|\omega)$  is computed from the neighborhood potential  $U(\mathbf{x}|\omega)$ , where the parameter  $\beta$  defines the magnitude of the contextual influence. For  $\beta = 0$  the influence is vanishing, and  $\beta = 1$  is a common choice [1,3,7].

### 3 The Iterative Algorithm

The probabilities and the necessary parameters are estimated during an iterative process using the current conditional probabilities (similar to the recently often used ICM algorithm (iterated conditional mode) [1]). In our case the conditional probabilities depend on the spectral and spatial features as set out above. At each iteration step and for each spectral band  $i$  we update the 'NoChange'-cluster center  $\mathbf{m}_i$  and its second principal axis  $\mathbf{g}_i$ , the change components  $\mathbf{c}_i$  and probabilities  $P(\omega|\mathbf{x})$  for each pixel, and re-estimate the typical scatter widths  $\sigma_{\omega,i}^2$  for both the 'NoChange' and the 'Change' cluster, and the probability sums  $N_\omega$ . The actual algorithm can be outlined as follows (see below Fig. 1):

For a given  $\beta$ , the iteration process converges to a local rather than a global maximum and thus depends on the initial labeling. Therefore we start the iteration with purely spectral features ( $\beta = 0$ ). In our experimental experience we have achieved fast convergence when the context-conditional probabilities are used with increasing influence. After starting with  $\beta = 0$  we proceed eventually towards  $\beta = 1$  as the relative number of yet converged pixel probabilities  $P(\omega|\mathbf{x})$  increases. So the spatial context information is introduced gradually to the iteration process, and spectral and spatial features are iterated at the same time.

### 4 Experimental Results on Simulated and Real Multitemporal Multispectral Imagery

The output of our unsupervised iterative algorithm is a binary image showing the locations of 'Change' pixels, and a float-type image giving the final probability  $P(\text{CH}|\mathbf{x})$  for each pixel.

The algorithm was verified on simulated test imagery with artificial 'Change' (Fig. 1) and two spectral bands of a real aerial image. These were duplicated and shifted by one pixel ('misregistration'); furthermore, an additive offset and a multiplicative rescaling of the gray values ('varying recording conditions') was applied separately to both bands; additive noise ( $\pm 5$  DC) and multiplicative noise (SNR = 5%) were superimposed; the 'Change' quadrangles were drawn into only one of the two spectral bands ('wavelength specific change').

The results on the simulated test imagery (Fig. 1) clearly show that only the combination of spectral features with local variance assessment and context-conditional probabilities yields optimal results.

We then applied the described change detection strategy to real multispectral image data, which was recorded by a DAEDALUS AADS 1268 line scanner during four campaigns from 1991 to 1995 in cooperation with the German Aerospace Research Establishment (DLR) at flight altitudes of 300 m and 1800 m (nadir ground resolution 70 cm and 4.2 m, respectively).

The multispectral images of 1991 and 1995 in Fig. 2 have  $n = 10$  spectral bands and were rectified and registered. The unsupervisedly detected changes were checked by eye appraisal against high resolving aerial photographs and show promising results; most changes are due to industrial construction activity between 1991 and 1995.

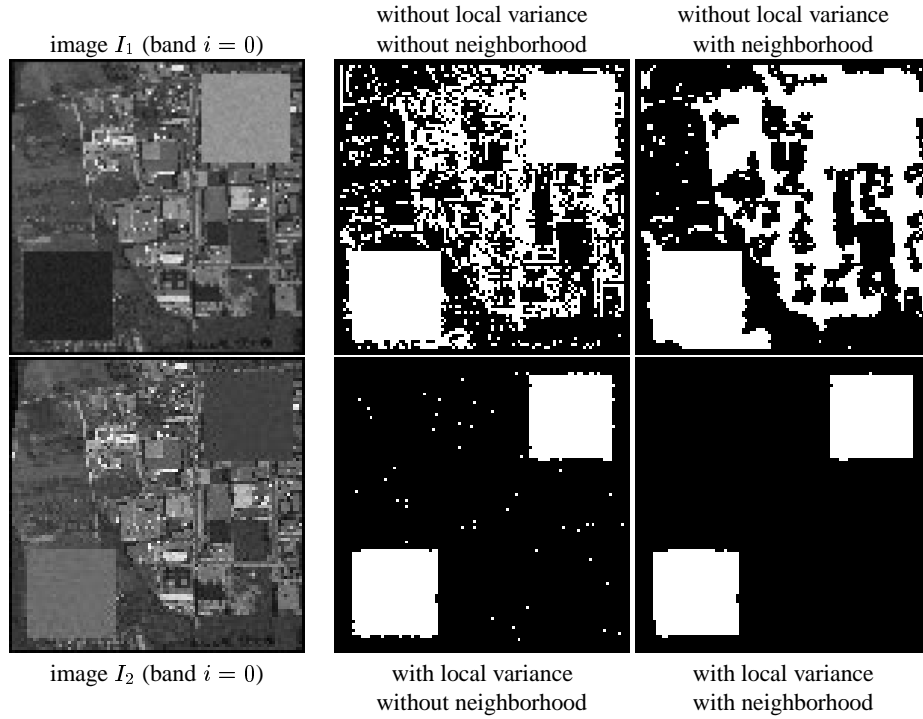


**Figure 1.** Change detection results on a simulated test image. Below: The iterative algorithm.

- 
0. register the two images  $I_1$  and  $I_2$  (rectification / geocoding)
  1. initialize the probabilities for all pixels to  $P(\omega|\mathbf{x}) = 0.5$ , where  $\omega = \{CH, NC\}$   
pre-compute the local spectral variance estimates  $\sigma_{loc,I_1,i}^2(\mathbf{x})$  and  $\sigma_{loc,I_2,i}^2(\mathbf{x})$  for all spectral bands  $i$  and all pixels  $\mathbf{x}$ 
    2. for all  $n$  spectral bands  $i$  do:
      - 2.1 determine principal axes from all pixels weighted with the current probabilities  $P(NC|\mathbf{x})$  and the inverse of the combined local variance  $\sigma_{loc,i}^2(\mathbf{x})$  in spectral band  $i$
      - 2.2 compute the 'Change'-components  $c_i(\mathbf{x}_i)$  and normalize them into  $c_i(\mathbf{x}_i)$  by dividing by the combined local variance in spectral band  $i$
      - 2.3 compute the CH- and NC-class-variances  $\sigma_{CH,i}^2$  and  $\sigma_{NC,i}^2$  from all pixels weighted with the current probabilities  $P(CH|\mathbf{x})$  and  $P(NC|\mathbf{x})$  respectively
      - 2.4 compute the spectral probability densities  $p_i(\mathbf{x}_i|CH)$  and  $p_i(\mathbf{x}_i|NC)$
    3. compute current context probabilities  $p_{con}(\mathbf{x}|CH)$  and  $p_{con}(\mathbf{x}|NC)$  from the current probabilities  $P(\omega|\mathbf{x})$
    4. compute current *a posteriori* probabilities  $P(\omega|\mathbf{x})$ , the new number of class members  $N_{CH}$  and  $N_{NC}$ , and the relative number of already having converged probabilities  $P(\omega|\mathbf{x})$
  5. exit if all probabilities  $P(\omega|\mathbf{x})$  have converged, else start over from (2)
-

## 5 Conclusions

We have addressed the problem of pixel-wise multispectral change detection in the framework of a Bayesian labeling problem, utilizing spectral features and spatial conditional probabilities derived from Markov random field modeling. The labeling decision on 'Change' or 'NoChange' is made with regard to maximum *a posteriori* probability for each pixel. The probabilities and the necessary parameters are estimated during an iterative process using the conditional probabilities (ICM: iterated conditional mode [1]). The here presented formulation of the change detection problem in a Bayesian labeling framework frees the problem from the need of arbitrary *ad hoc* thresholds, and delivers meaningful change probability values as well as error probabilities of first and second kind. Certainly, for a specific monitoring application, particularly useful weights of the various spectral bands may be experimentally found by the experienced analyst and hand-tuned thresholds may prove successful. However, just as unsupervised clustering and labeling of multispectral imagery is used complementarily to costly analyst-trained classifiers, our unsupervised change detection approach can provide a primary and well founded tool for change detection. Our approach uses all spectral information on equal footing and is robust in so far as it particularly addresses a number of well known problems of multispectral change detection:

- varying illumination and recording conditions
- small misregistration errors
- (often unemployed) contextual information
- unknown threshold parameters
- additive and multiplicative noise

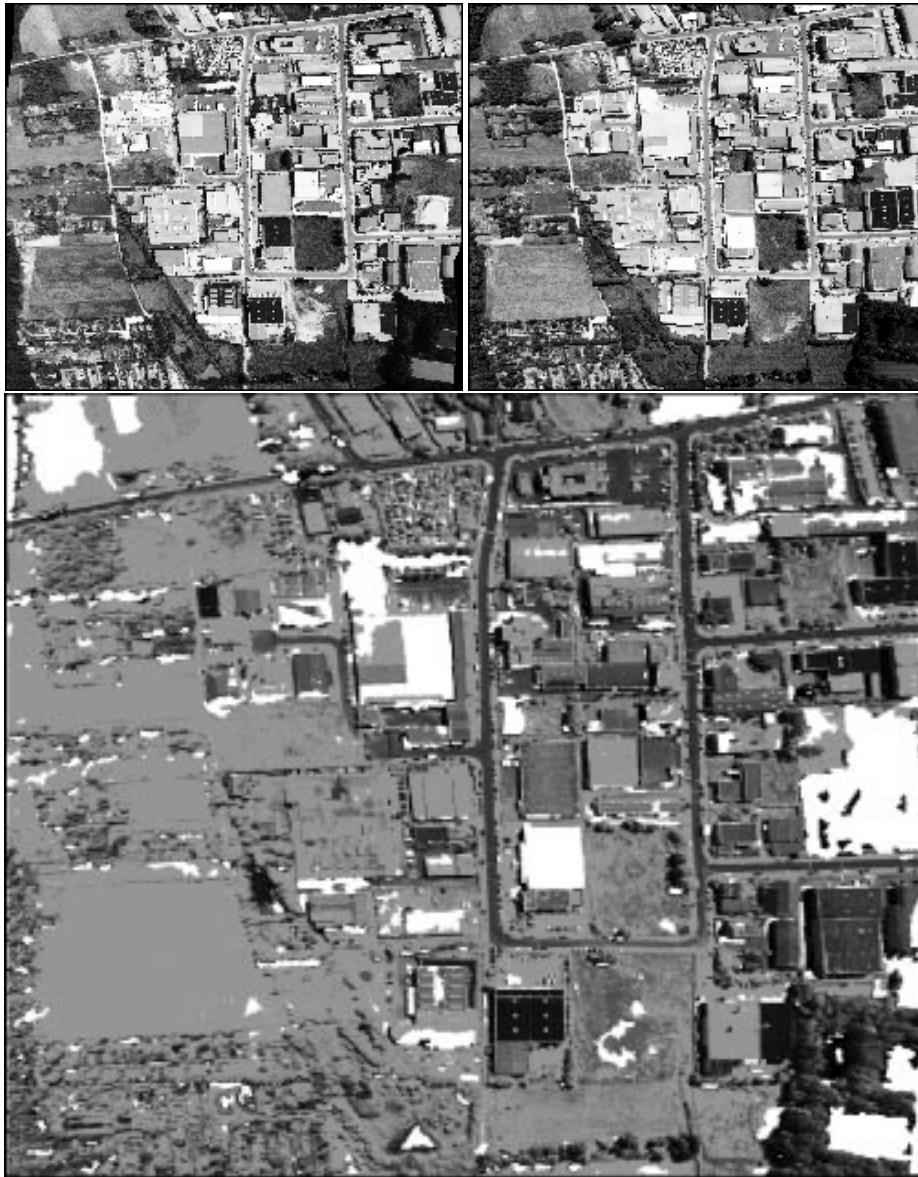
Promising results were achieved on simulated test imagery as well as on real multi-temporal, remotely sensed multispectral imagery. We found that the combination of spectral features with local variance and neighborhood potentials delivers a substantial improvement.

## References

1. J. Besag. On the statistical analysis of dirty pictures. *Journal of the Royal Statistical Society B*, 48(3):259–302, 1986.
2. R. O. Duda and P. E. Hart. *Pattern Classification and Scene Analysis*. Wiley, New York, 1973.
3. Y. Jung and Philip H. Swain. Bayesian contextual classification based on modified *M*-estimates and Markov random fields. *IEEE T.o.Geosci.a.Rem.Sens.*, 34(1):67–75, 1996.
4. S.Z. Li. *Markov Random Field Modeling in Computer Vision*. Springer, Tokyo, 1995.
5. J. A. Richards. *Remote Sensing Digital Image Analysis*. Springer, New York, 1993.
6. A. Singh. Review article: Digital change detection techniques using remotely-sensed data. *International Journal of Remote Sensing*, 10(6):989–1003, 1989.
7. A.H.S. Solberg, T. Taxt, and A.K. Jain. A markov random field model for classification of multisource satellite imagery. *IEEE T.o.Geosci.a.Rem.Sens.*, 34(1):100–113, 1996.
8. R. Wiemker, K. Rohr, L. Binder, R. Sprengel, and H.S. Stiehl. Application of elastic registration to imagery from airborne scanners. In *Proceedings of the XVIII. Congress of the International Society for Photogrammetry and Remote Sensing ISPRS 1996, Vienna*, volume XXXI part B4 of *International Archives of Photogrammetry and Remote Sensing*, pages 949–954, 1996.

1991

1995



'Change' coded in white

**Figure 2.** Change detection between two registered multispectral aerial images recorded in 1991 (top left) and 1995 (top right) of an industrial suburb of Nürnberg (rectified scanner image with 10 spectral bands,  $1000 \times 800$  pixels). Bottom: 'Change'-areas are color-coded white on a gray image background. The neighborhood was defined as a  $5 \times 5$  window.